Journal of Magnetic Resonance **150,** 184–193 (2001)
doi:10.1006/jmre.2001.2331, available online at http://www.idealibrary.com on IDEAL®

Dipolar and *J* Encoded DQ MAS Spectra under Rotational Resonance

C. Filip,* X. Filip,† M. Bertmer,* D. E. Demco,* and B. Blümich*,[1]

*Institute for Technical Chemistry and Macromolecular Chemistry, RWTH Aachen, Worringerweg 1, D-52074 Aachen, Germany; and †Institute of Isotopic and Molecular Technology, P.O. Box 700, R-3400 Cluj, Romania

Received December 8, 2000; revised March 22, 2001

A two-dimensional (2D) double-quantum (DQ) experiment under rotational resonance (R^2) conditions is introduced for evaluating dipolar couplings in rotating solids. The contributions from the R^2-recoupled dipolar interaction and the *J* coupling can be conveniently separated in the resulting 2D R^2-DQ spectrum, so that the unknown dipolar coupling can readily be extracted, provided that the values of the involved *J* coupling constants are known. Since the measured parameters are integral intensity ratios between suitably chosen absorption peaks in the 2D spectrum, the proposed method is characterized by a reduced sensitivity to relaxation parameters. The effect of rotor-modulated terms, including chemical shift anisotropy, is efficiently averaged out by synchronizing the excitation/reconversion time with the rotor period. All of these features are demonstrated theoretically by the example of two model systems, namely, isolated spin-pairs and a three-spin system. The results of the theoretical models are applied to both ^{13}C and ^{1}H nuclei to extract dipolar couplings in uniformly ^{13}C labeled L-alanine and a crosslinked natural rubber.

Key Words: **solid-state NMR; magic angle spinning; rotational resonance; double-quantum NMR.**

1. INTRODUCTION

The investigation of local structure by solid state nuclear magnetic resonance (NMR) often requires recoupling (*1*) of weak dipolar interactions, which otherwise are efficiently averaged out by magic angle spinning (MAS) (*2, 3*). In addition to radiofrequency techniques (*4–12*), in homonuclear systems recoupling methods also have been developed (*13–17*) that exploit the so-called rotational resonance (R^2) phenomenon (*19*). By this, one can selectively reintroduce part of the dipolar interaction between two chemically distinct nuclear sites, j and k, provided that their isotropic chemical shift difference matches a small integer multiple of the rotor frequency, i.e., $\delta_{jk} = \omega_j - \omega_k = n\omega_R$. So far the R^2 recoupling techniques have been applied on dilute nuclear spin probes, particularly ^{13}C and ^{15}N, because the high spectral resolution needed for the observation of the R^2 phenomenon is easily achievable in such systems with inhomogeneous line broadening (*20*) and also because of the important applications of these nuclei in the structural elucidation of complex biological molecules (*21–24*).

The main features under rotational resonance, i.e., enhanced magnetization exchange and line splitting and broadening (*25–27*), are all used for measuring dipolar couplings and, hence, internuclear distances. The dipolar coupling between two resonant nuclei can readily be extracted from the decay of magnetization exchange curves and from the splitting of single-quantum (SQ) or double-quantum (DQ) filtered lines, in experiments suitably designed to exploit one or the other of these features.

In the conventional approach, quasi-isolated spin-pairs are engineered by specific isotopic labeling of nonequivalent molecular sites, so that spin systems with very simple spin dynamics are determined, which can readily be manipulated. If a *differential longitudinal magnetization* is first prepared by selective inversion of one resonance, the dynamics simplifies even further, because this initial state is expected to evolve solely under the recoupled dipolar interaction. Such a strategy is employed in R^2 magnetization exchange (*14, 15*) and DQ filtering experiments (*16*). The simplicity of this concept is, however, spoiled in practice, because both methods also prove to be quite sensitive to relaxation parameters, in addition to the measured dipolar coupling. In particular, the strong dependence on the $T_{2,ZQ}$, the relaxation time of the zero-quantum coherences, limits the accuracy of distance measurements by these methods to such values for which the decay of the magnetization exchange signal, or the splitting of the DQ filtered line, become smaller than the $T_{2,ZQ}$-induced decay, or line broadening, respectively.

Therefore, the development of efficient techniques by which the effect of relaxation can be conveniently handled is highly desirable. Such alternative methods have already been proposed in the case of R^2 magnetization exchange. For instance, in the recently developed R^2-tickling experiment (*14*), the sensitivity to $T_{2,ZQ}$ is greatly reduced, which enables accurate distance evaluation up to 5–6 Å in ^{13}C-labeled compounds. In the present work we show that the disturbing effect of relaxation can be reduced in R^2-DQ experiments as well. Unlike the case presented in Refs. (*16, 17*), the *transverse magnetization* is employed here as an initial state, which is then converted into DQ coherences using an excitation scheme similar to that reported in Ref. (*13*). Nevertheless, different from both methods (*13, 16*), the measured

[1] To whom correspondence should be addressed. Fax: ++49 241 8888 185. E-mail: bluemich@mc.rwth-aachen.de.

1090-7807/01 $35.00

parameters are *integral intensity ratios* between suitably chosen absorption lines in a two-dimensional (2D) R^2-DQ spectrum.

Although the spin system response is more complex now, because the J coupling interaction also contributes to the spin dynamics and generally a smaller efficiency in the DQ excitation process is obtained, the strategy proposed here has important advantages, namely (i) the absorption peaks originating from J coupling and dipolar interaction are separated from each other in the resulting 2D spectrum, so that one can determine dipolar couplings from their intensity ratio, provided that the values of the involved J couplings are known from solution spectra, (ii) the method is not restricted to isolated spin-pairs, but can be applied to multispin systems as well as that discussed in Refs. (*13–17*), (iii) the influence of relaxation can be greatly reduced, which increases the accuracy in evaluating dipolar couplings, and (iv) the effect of the remaining rotor-modulated terms, including chemical shift anisotropy (CSA), is efficiently averaged out under fast MAS and also by rotor synchronizing the excitation/reconversion times.

All of these features have been demonstrated theoretically on two model systems, namely isolated spin-pairs and a three-spin system. The theoretical results are used to extract dipolar couplings from the 2D R^2-DQ spectra recorded on ^{13}C in uniformly labeled L-alanine, and on ^1H, in a crosslinked natural rubber. To our knowledge, no R^2-induced line splitting on protons has been reported so far, although the basic condition for employing the R^2 phenomenon, i.e., an inhomogeneous-like broadening, is fulfilled in such systems with strong molecular motion. Here one shows that the application of rotational resonance on protons is feasible, and the proposed DQ experiment constitutes an efficient method for estimating small dipolar couplings between different chemical moieties in soft solids.

2. EXPERIMENTAL

The experiments were performed on a Bruker DSX 500 NMR spectrometer operating at 500.45 and 125.85 MHz for ^1H and ^{13}C resonance frequencies, respectively. The DQ spectra were obtained employing the pulse sequence which is depicted in Fig. 1. The excitation of the DQ coherences is obtained using the nonselective two-pulse sequence, where an additional central π-pulse eliminates the frequency-offset dependence of the DQ signal (Fig. 1b). This pulse divides the full excitation time into two equal periods of $\tau = N\tau_R$, with N an integer and τ_R the rotor period. For reconversion of the DQ coherences to observable magnetization, a similar pulse-sequence is used, but with a $\pi/2$ phase shift of its pulses. For recording 2D DQ spectra the TPPI procedure, combined with a four-step phase cycling of the excitation pulses (*12*), was used. No cross-polarization was applied in the case of ^{13}C spectra, only dipolar decoupling on the proton channel.

The investigated spin systems are represented by protons of various functional groups in a crosslinked natural rubber and carbons in uniformly ^{13}C labeled L-alanine, diluted 1:10 in the unlabeled compound. Both are well-characterized compounds and thus can be used to test the performance of the proposed method.

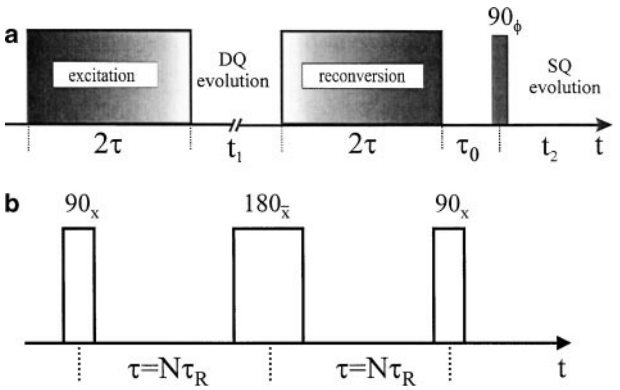

FIG. 1. (a) Schematic representation of the 2D DQ MAS experiment. This basic scheme can be used with different excitation/reconversion pulse sequences. The z-filter is represented by a rotor-synchronized purging period τ_0 (inserted delay between reconversion and detection to allow undesired coherences to decay). (b) The pulse sequence used for exciting DQ coherences. For reconversion a similar pulse sequence was used, except that the phases were shifted by $\pi/2$.

The DQ experiment described above was performed at those R^2 conditions for which no R^2-induced line splitting was obtained in conventional SQ spectra. Specifically, this refers to the $n = 1$ rotational resonance condition with respect to the COOH–CH_3 lines ($\nu_R = 19.8$ kHz) in the case of carbons and with respect to the CH–CH_2 lines ($\nu_R = 1.53$ kHz) and the CH–CH_3 lines ($\nu_R = 1.74$ kHz) in the case of protons, respectively. The resulting 2D R^2-DQ spectra are illustrated in Figs. 2 and 3. To simplify the presentation, the COOH, CH, and CH_3 carbon and CH, CH_2, and CH_3 proton resonance frequencies are designated in the following by ω_1, ω_2, and ω_3. Also, the notations $\sigma_{jk} = \omega_j + \omega_k$ and $\delta_{jk} = \omega_j - \omega_k$ are used.

Figure 2a shows the ^{13}C R^2-DQ spectrum recorded at $2\tau = 52\tau_R$ and $\nu_R = \delta_{13}$. As can be seen from this figure, the nuclei which are subjected to rotational resonance give rise to a four-peak pattern, with the peaks symmetrically displaced by $\pm\delta_{13}$ with respect to the mean frequency, σ_{13}, in the DQ dimension. Their origin in the R^2-recoupled dipolar interaction is clearly demonstrated by the DQ spectrum presented in Fig. 2b. The same experimental conditions were employed here, except that ν_R was set to 20.8 kHz. Although this spinning frequency corresponds to only 1 kHz away from rotational resonance, one can see that the four-peak pattern has completely vanished. In both spectra one also obtains two pairs of absorption peaks, located at (ω_1, ω_2) and (ω_1, ω_3) along the SQ dimension and at σ_{12} and σ_{23} along the DQ dimension, respectively. Since their spectral positions do not change upon changing the spinning frequency, obviously these four peaks are determined by an interaction which is not affected by MAS, that is, the J coupling. Such an interpretation fits very well with the known values of the carbon–carbon J coupling constants in L-alanine, namely $J_{COOH-CH} = 55$ Hz, $J_{CH-CH_3} = 35$ Hz, and $J_{COOH-CH_3} < 5$ Hz (*28*). According

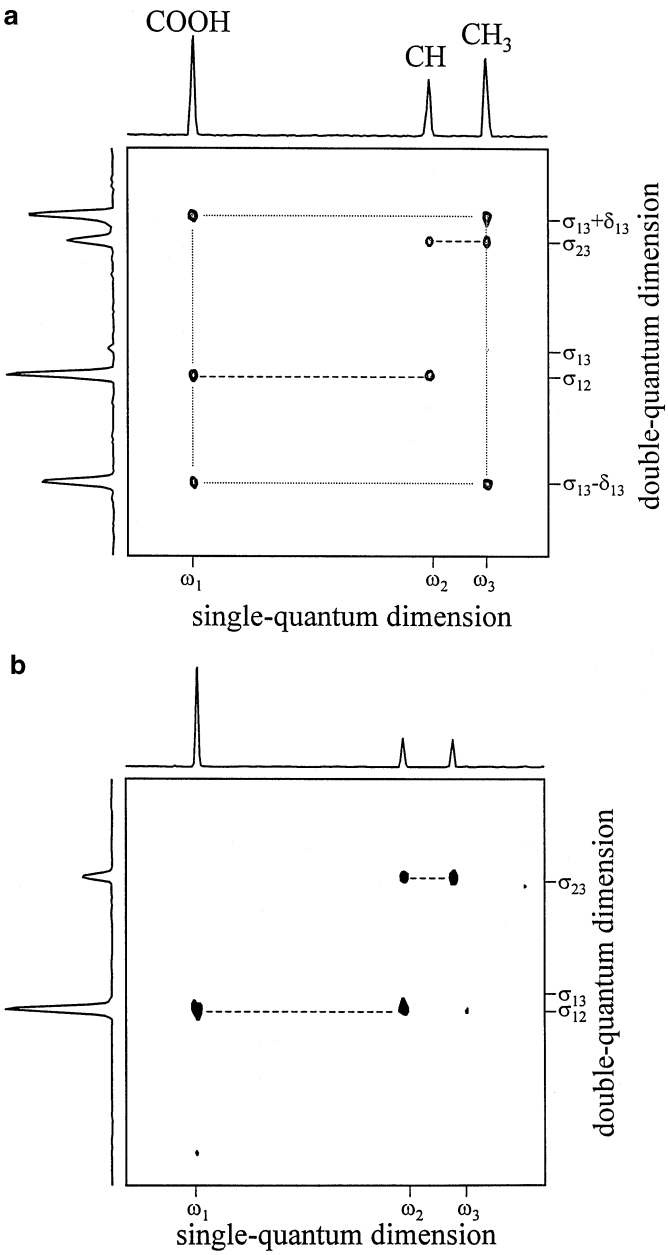

FIG. 2. (a) The 2D R^2-DQ spectrum of ^{13}C in uniformly labeled L-alanine, obtained at $\nu_R = \delta_{13} = 19.8$ kHz ($n = 1$ R^2 condition corresponding to the COOH–CH_3 lines), using a total excitation time of $2\tau = 52\tau_R = 2.62$ ms. The notations ω_1, ω_2, and ω_3 along the SQ dimension represent the ^{13}C resonance frequencies of the COOH, CH, and CH_3 carbons. Along the DQ dimension, $\sigma_{jk} = \omega_j + \omega_k$ and $\delta_{jk} = \omega_j - \omega_k$. (b) Similar to case (a), except that $\nu_R = 20.8$ kHz, i.e., 1 kHz away from the corresponding R^2 condition.

to this picture, one can explain also the small absorption line located at σ_{13} in the DQ dimension (Fig. 2a): this is determined by the $J_{COOH–CH_3}$ coupling. This demonstrates the sensitivity of the proposed DQ experiment, by which even the effect of such small interactions can be identified in the resulting spectrum.

A similar behavior was found in the proton spectra as well. Figure 3 shows the ^1H R^2-DQ spectra recorded with a total excitation time of $2\tau = 16\tau_R$ at the spinning frequencies $\nu_R = \delta_{12}$ (Fig. 3a) and $\nu_R = \delta_{13}$ (Fig. 3b). The symmetric four-peak pattern, determined by the corresponding R^2 recoupled dipolar interaction, is obtained also in this case. Different from carbon spectra, however, only one pair of J lines occurs here, which correlates to the CH–CH_2 protons. This can be understood based on the very small values of the other two J coupling constants,

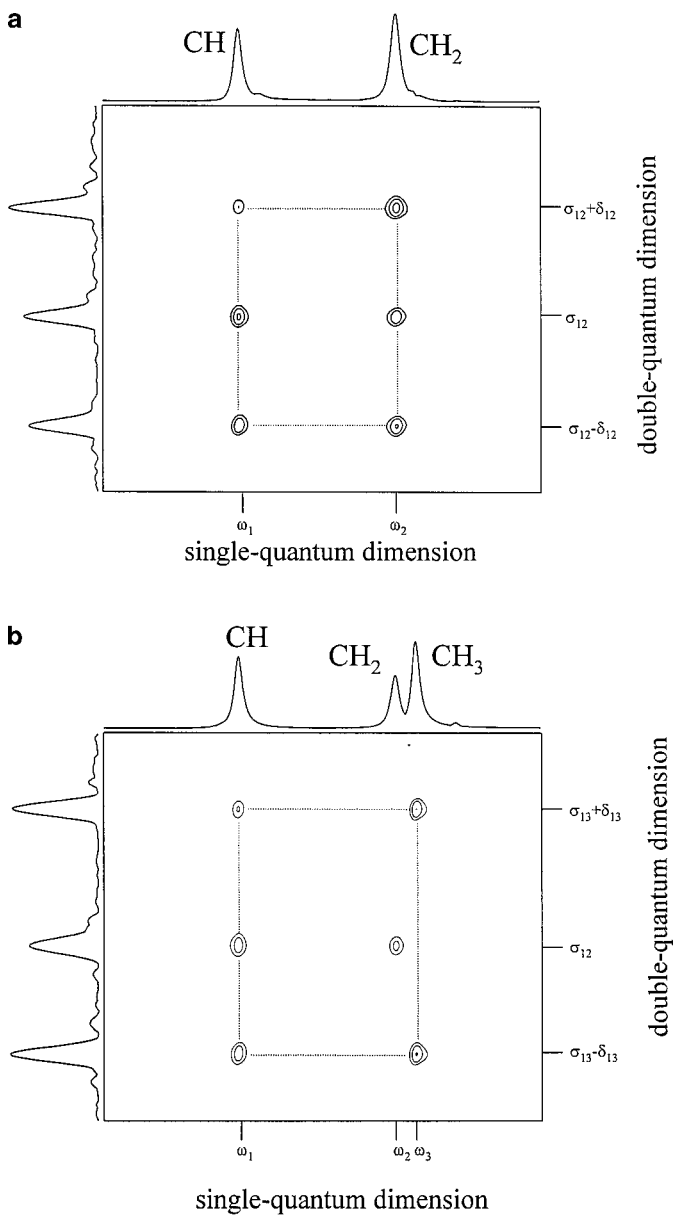

FIG. 3. (a) The 2D R^2-DQ spectrum of ^1H in a crosslinked natural rubber (phr = 1), obtained at $\nu_R = \delta_{12} = 1.53$ kHz ($n = 1$ R^2 condition corresponding to the CH–CH_2 lines), using a total excitation time of $2\tau = 16\tau_R = 10.46$ ms. The notations ω_1, ω_2, and ω_3 along the SQ dimension represent the ^1H resonance frequencies of the CH, CH_2, and CH_3 protons. Along the DQ dimension, $\sigma_{jk} = \omega_j + \omega_k$ and $\delta_{jk} = \omega_j - \omega_k$. (b) Similar to case (a), except that the $n = 1$ R^2 condition corresponding to the CH–CH_3 lines is employed now ($\nu_R = \delta_{13} = 1.74$ kHz).

compared with $J_{\mathrm{CH-CH_2}}$. As an estimation of the relative strengths between the relevant J couplings in natural rubber, one can take, for instance, the typical values of the J coupling constants between protons in similar structural arrangements in liquids, i.e., ${}^3J_{\mathrm{CH-CH_2}} \simeq 10$ Hz, ${}^4J_{\mathrm{CH-CH_3}} < 3$ Hz, and ${}^4J_{\mathrm{CH_2-CH_3}} < 1$ Hz (*29*).

Apart from this intuitive explanation of the experimental results, however, a theoretical analysis is needed for explicitly relating the spectral parameters with interaction parameters characteristic to the investigated system. Such a theory, together with its application for a quantitative analysis of the measured R^2-DQ spectra, is provided in the following sections.

3. THEORY

The 2D R^2-DQ experiment presented above is analyzed under the assumption that the main features of the resulting spectra are determined by the static part of the spin Hamiltonian expressed into an interaction picture with respect to the isotropic chemical shift interaction. In the Liouville space this is defined by

$$\rho_I(t) = e^{i\hat{\mathcal{H}}_{\mathrm{CS}}t}\rho(t), \qquad [1]$$

where $\rho(t)$ and $\rho_I(t)$ are the Schrödinger and the interaction picture representations of the density operator, while

$$\mathcal{H}_{\mathrm{CS}} = \sum_j \omega_j I_{jz} \qquad [2]$$

is the isotropic chemical shift (CS) Hamiltonian. Under these conditions, the truncated spin Hamiltonian reads

$$\mathcal{H}_{0,I} = -\frac{1}{2}\omega^{\mathrm{D}}_{JK}\left(b^{JK}_1 I_{J+}I_{K-} + b^{JK}_{-1} I_{J-}I_{K+}\right) + \sum_{j,k}(2\pi J_{jk})I_{jz}I_{kz}, \qquad [3]$$

where $\omega^{\mathrm{D}}_{JK} = \frac{\mu_0\gamma^2\hbar^2}{4\pi r^3_{JK}}$ and J_{jk} are the dipolar and J coupling constants between the specified nuclei, with r_{JK} the internuclear distance, while the functions $b^{JK}_{\pm 1} = (\sqrt{2}/4)\sin(2\beta_{JK})\cdot\exp(\pm\alpha_{JK})$ depend on the polar angles $(\alpha_{JK}, \beta_{JK})$, which give the orientation of the dipolar tensor with respect to the rotor axis. The summation indices run over all possible spin pairs (j, k) in the case of the J coupling interaction, while the labels (J, K) refer specifically to those nuclei which are subjected to rotational resonance.

In order to evaluate the NMR signal

$$S(t) = \langle I_+ \mid \rho(t)\rangle = \langle I_+ \mid \hat{U}(t,0) \mid \rho(0)\rangle, \qquad [4]$$

the density operator or, equivalently, the time propagator $\hat{U}(t, 0)$, should be brought back to the Schrödinger representation. This is achieved by the transformation

$$\hat{U}(t,t') = e^{-i\hat{\mathcal{H}}_{\mathrm{CS}}t}\hat{U}_I(t,t')\,e^{i\hat{\mathcal{H}}_{\mathrm{CS}}t'}, \qquad [5]$$

where t and t' are two arbitrary moments of time and where

$$\hat{U}_I(t,t') = e^{-i\hat{\mathcal{H}}_{0,I}(t-t')}. \qquad [6]$$

In Eq. [4], $\hat{U}(t, 0)$ is replaced by the product $\hat{U}^{\mathrm{SQ}}_{\mathrm{ev}}\hat{U}_{\mathrm{rec}}\hat{U}^{\mathrm{DQ}}_{\mathrm{ev}}\hat{U}_{\mathrm{ex}}$ of the propagators corresponding to the four distinct time periods of the experiment, namely excitation, DQ evolution, reconversion, and SQ evolution, respectively. Wherever necessary, they include also the action of the corresponding radiofrequency pulses, as shown in Fig. 1. The DQ filtration through phase cycling is accounted for by selecting only DQ terms in the excitation period, while in order to incorporate the TPPI procedure used for the DQ evolution, any periodic function in t_1 was converted to only one trigonometric function (for instance, here we have chosen the cosine function).

The DQ spectra obtained under different experimental conditions are analyzed below by evaluating the integral intensities of the absorption lines, whose values primarily reflect the evolution under the Hamiltonian $\mathcal{H}_{0,I}$ during the excitation and reconversion periods. Therefore, the excitation and reconversion propagators are taken in the form given by Eq. [5], while in the expressions for $\hat{U}^{\mathrm{SQ}}_{\mathrm{ev}}$ and $\hat{U}^{\mathrm{DQ}}_{\mathrm{ev}}$ only the evolution under the isotropic CS is considered. Using this procedure, in the following we evaluate the integral intensities of the resulting 2D R^2-DQ spectra for two different spin configurations with relevance from both theoretical and practical points of view.

3.1. Isolated Spin-Pairs

The study of this system is important because it represents the so far most widely used spin configuration in R^2 experiments, and also, based on this simple example, one can more easily identify those features which are general to all R^2-DQ spectra, irrespective of the particular system that is investigated. For instance, applying the relation [5] to the spin-pair case one obtains $\hat{U}_{\mathrm{ex}}(2\tau, 0) = \hat{P}_{90}(x)\hat{U}'_{\mathrm{ex}}(2\tau,\tau)\hat{P}_{180}(-x)\hat{U}'_{\mathrm{ex}}(\tau,0)\hat{P}_{90}(x)$, with

$$U'_{\mathrm{ex}}(\tau,0) = \exp[-i(2\pi J I_{1z}I_{2z})\tau]\exp\left[i\frac{\omega^{\mathrm{D}}_{12}}{2}\left(b^{12}_1 e^{i\delta_{12}\tau}I_{1+}I_{2-} + b^{12}_{-1}e^{-i\delta_{12}\tau}I_{1-}I_{2+}\right)\tau\right]. \qquad [7]$$

Thus, the dipolar part of the excitation propagator depends explicitly on the excitation time τ, unless it is synchronized with the rotor period, i.e., $\tau = N\tau_{\mathrm{R}}$. In such a case one has $\tau_{\mathrm{R}} = 2N\pi/\delta_{12}$, and the modulation factors in the relationship above vanish. On the other hand, the dipolar terms in the reconversion propagator,

$$U'_{\mathrm{rec}}(\tau + t_1, t_1) \sim \exp\left[i\frac{\omega^{\mathrm{D}}_{12}}{2}\left(b^{12}_1 e^{i\delta_{12}t_1}I_{1+}I_{2-} + b^{12}_{-1}e^{-i\delta_{12}t_1}I_{1-}I_{2+}\right)\right], \qquad [8]$$

still preserve a phase factor, $e^{\pm i\delta_{12}t_1}$, which depends on t_1, the DQ evolution time. This dependence is, however, advantageous, because it enables one to separate along the DQ dimension the absorption lines determined by the R^2 recoupled dipolar interaction from those generated by J coupling. Such a mechanism is similar to the mechanism of sideband generation by rotor encoding during the reconversion period, which was found previously in MQ MAS spectra (*12*).

Besides the coherent evolution determined by the propagators above, one has also to take into account the effect of relaxation. This can be done in a phenomenological way by multiplying the excited spin coherences with suitable relaxation functions, $R_j(t-t') = \exp[-(t-t')/T^*_{2,j}]$. Corresponding to our experimental conditions, $T^*_{2,j}$ refers to the effective transverse relaxation time of single-quantum coherences, since only such coherences evolve before the application of the last pulse in the excitation / reconversion period. For generality, we also consider the case when each distinct chemical site j is characterized by its one relaxation time, $T^*_{2,j}$. However, the use of this simplified model is restricted to the case when the difference between the relaxation times corresponding to the R^2 recoupled sites is relatively small (*30*).

Including now both effects, and confining our attention to DQ terms, the expression of the density operator at the end of the excitation period reads

$$\rho(2\tau) \sim \mathrm{DQ}_{12}[\sin(2\pi J\tau)\cos(\omega_{12}\tau) - \cos\alpha_{12}\cos(2\pi J\tau)\sin(\omega_{12}\tau)], \quad [9]$$

with $\omega_{12} = \omega^{\mathrm{D}}_{12} b^{12}_{(1)}$ and $\mathrm{DQ}_{12} = \frac{1}{2i}(I_{1+}I_{2+} - I_{1-}I_{2-})[R_1(2\tau) + R_2(2\tau)]$. A similar expression can be derived also if the reconversion propagator is considered instead, except that $\cos\alpha_{12}$ must be replaced by $\cos(\alpha_{12} + \delta_{12}t_1)$. Inserting this into relation [4], the finally obtained result for the NMR signal reads

$$S(t_2, t_1) = \sum_{p=1,2}\sum_{q=1}^{3} I_{p,q} e^{i\omega_p t_2}\cos(\Omega_q t_1). \quad [10]$$

Its Fourier transform constitutes a pattern of six absorption peaks, located at ω_1 and ω_2 along the SQ dimension, and at $\Omega_1 = \sigma_{12} - \delta_{12}$, $\Omega_2 = \sigma_{12}$, and $\Omega_3 = \sigma_{12} + \delta_{12}$ along the DQ dimension, respectively. The amplitude factors $I_{p,q}$ correspond to their integral intensities and are given by

$$\begin{aligned} I_{1,1} &= I_{1,3} = \frac{1}{8} I(0) R_2(2\tau)\cos^2(2\pi J\tau)\langle\sin^2(\omega_{12}\tau)\rangle \\ I_{2,1} &= I_{2,3} = \frac{1}{8} I(0) R_1(2\tau)\cos^2(2\pi J\tau)\langle\sin^2(\omega_{12}\tau)\rangle \\ I_{1,2} &= \frac{1}{2} I(0) R_1(2\tau)\sin^2(2\pi J\tau)\langle\cos^2(\omega_{12}\tau)\rangle \\ I_{2,2} &= \frac{1}{2} I(0) R_2(2\tau)\sin^2(2\pi J\tau)\langle\cos^2(\omega_{12}\tau)\rangle, \end{aligned} \quad [11]$$

where

$$I(0) = I_1(0)R_1(2\tau) + I_2(0)R_2(2\tau), \quad [12]$$

with $I_1(0)$ and $I_2(0)$ the integral intensities of the two lines in the corresponding SQ spectrum and where $\langle\cdots\rangle$ represents the powder average.

Two limiting cases have to be distinguished now, namely $\omega^{\mathrm{D}}_{12} \to 0$, for which $I_{1,1} = I_{1,3} = I_{2,1} = I_{2,3} = 0$, and $J \to 0$ where $I_{1,2} = I_{2,2} = 0$. This indicates that the four absorption lines located at $\sigma_{12} \pm \delta_{12}$ along the DQ dimension originate from the R^2 recoupled dipolar interaction, while the other two lines at σ_{12} are determined by the J coupling. Correspondingly, in the following they will be referred to as the dipolar and the J lines, respectively.

Apart from the two extremes, however, the integral intensities of all these lines are encoded by both interactions and thus can be used for evaluation of the dipolar coupling. For this purpose, the J coupling is approximated by its value determined from NMR spectra in solution, so that only the dependence on relaxation parameters remains. This can also be removed by adding the two DQ slices and then taking the ratio between the dipolar and J lines, i.e.,

$$\eta = \frac{I_{1,1} + I_{2,1}}{I_{1,2} + I_{2,2}} = \frac{1}{4}\frac{\cos^2(2\pi J\tau)\langle\sin^2(\omega_{12}\tau)\rangle}{\sin^2(2\pi J\tau)\langle\cos^2(\omega_{12}\tau)\rangle}. \quad [13]$$

The above result shows us that even in the most general case when the relaxation times associated to different chemical sites are not equal to each other, one can still find a parameter whose value *is independent of relaxation* and thus can be used for an accurate evaluation of the dipolar coupling.

However, this conclusion is no longer valid when the difference between the relaxation times (or linewidths) of the resonant sites is comparable with the measured dipolar coupling. In such cases, ω_{12} in Eq. [13] must be replaced by $(\omega^2_{12} - \Delta^2)^{1/2}$, with $\Delta = \frac{1}{T^*_{2,1}} - \frac{1}{T^*_{2,2}}$ (*30*). Thus, a small dependence on relaxation parameters still remains in this case, which in practice can be taken into account, for instance, by replacing Δ with the difference between the corresponding linewidths. Nevertheless, more elaborate models are needed when such line broadening differences come primarily from the incomplete proton decoupling (*30*). Therefore, an accurate evaluation of dipolar couplings by this method requires either efficient decoupling techniques or an adequate theoretical treatment of the residual heteronuclear interaction.

3.2. The Three-Spin Model

Using this example, one can explicitly show the complications by going from the classical spin-pair approach to a multispin system. Also, the three-spin case is important for practical applications: in the case of ^{1}H nuclei one always deals with multispin systems, while in the case of ^{13}C techniques, the

tendency now is to employ uniformly labeled compounds instead of the more expensive compounds selectively labeled at specific molecular positions.

Corresponding to the experimental conditions employed to acquire the ^{13}C R^2-DQ spectra, first one considers the following interaction parameters: the resonance frequencies of the involved spins are all different from each other, with $|\omega_1| < |\omega_2| < |\omega_3|$, $J_{12} \neq J_{23} \neq 0 \neq J_{12}$, $J_{13} \simeq 0$, and $\omega_R = \delta_{13}$. The theoretical analysis follows exactly the same steps as in the spin-pair case, so that no further details about the calculation are needed. Here, we only mention that the expression of the resulting NMR signal is similar to that in Eq. [10], except that one obtains three DQ slices now ($p = 1, 2, 3$), and also the structure of each slice along the DQ dimension is more complex. Specifically, the 2D R^2-DQ spectrum is made up of 17 peaks. However, not all of them are equally important. For instance, the dominant eight lines in this pattern can be easily understood based on the previous example, since their spectral positions along the DQ dimension, $\Omega_1 = \sigma_{13} - \delta_{13}$, $\Omega_2 = \sigma_{12}$, $\Omega_3 = \sigma_{23}$, and $\Omega_4 = \sigma_{13} + \delta_{13}$, can be correlated with the particular interactions they originate from. The corresponding integral intensities are given by

$$
\begin{aligned}
I_{1,1} &= I_{1,4} = \frac{1}{8}\langle A^2\rangle R_1(2\tau)[I_1(0)R_1(2\tau) + I_3(0)R_3(2\tau)] \\
I_{3,1} &= I_{3,4} = \frac{1}{8}\langle A^2\rangle, R_3(2\tau)\,[I_1(0)R_1(2\tau) + I_3(0)R_3(2\tau)] \\
I_{1,2} &= \frac{1}{2}\left[\langle B_+^2\rangle I_1(0)R_1^2(2\tau) + \frac{1}{2}\langle B_+C_+\rangle R_1(2\tau)I_2(0)R_2(2\tau)\right] \\
I_{3,3} &= \frac{1}{2}\left[\langle B_-^2\rangle I_3(0)R_3^2(2\tau) + \frac{1}{2}\langle B_-C_-\rangle R_3(2\tau)I_2(0)R_2(2\tau)\right] \\
I_{2,2} &= \frac{1}{8}\big[\langle C_+^2\rangle I_2(0)R_2^2(2\tau) + 2\langle B_+C_+\rangle I_1(0)R_1(2\tau)R_2(2\tau)\big] \\
I_{2,3} &= \frac{1}{8}\big[\langle C_-^2\rangle I_2(0)R_2^2(2\tau) + 2\langle B_-C_-\rangle I_3(0)R_3(2\tau)R_2(2\tau)\big],
\end{aligned}
\qquad [14]
$$

with the coefficients

$$
\begin{aligned}
A &= \frac{\omega_{13}}{\omega}\cos(2\pi J_\sigma\tau)\sin(\omega\tau) \\
B_\pm &= \sin(2\pi J_\sigma\tau)\cos(\omega\tau) \pm \frac{2\pi J_\delta}{\omega}\cos(2\pi J_\sigma\tau)\sin(\omega\tau) \\
C_\pm &= \sin(4\pi J_\sigma\tau) \pm \frac{2\pi J_\delta}{\omega_{13}}\sin(\omega_{13}\tau),
\end{aligned}
\qquad [15]
$$

where $J_\sigma = 1/2(J_{12} + J_{23})$ and $J_\delta = 1/2(J_{12} - J_{23})$, and

$$
\omega = \left[4\pi^2 J_\delta^2 + \frac{1}{8}\sin^2(2\beta_{13})\left(\omega_{13}^{\mathrm{D}}\right)^2\right]^{1/2}. \qquad [16]
$$

In analogy to the spin-pair case, one can show that the first four lines are dipolar lines, while the last four are J lines, respectively.

The spectral positions along the DQ dimension, $\Omega_{5,6} = \sigma_{12} \pm \delta_{13}$, $\Omega_{7,8} = \sigma_{23} \pm \delta_{13}$, and $\Omega_9 = \sigma_{13}$, of the other nine peaks no longer fit into such a correlation scheme. Their integral intensities,

$$
\begin{aligned}
I_{1,5} &= I_{1,6} = \frac{1}{8}\big[\langle D^2\rangle I_3(0)R_3^2(2\tau) - \langle DE\rangle I_2(0)R_3(2\tau)R_2(2\tau)\big] \\
I_{2,5} &= I_{2,6} = \frac{1}{8}\big[\langle E^2\rangle I_2(0)R_2^2(2\tau) - \langle DE\rangle I_3(0)R_3(2\tau)R_2(2\tau)\big] \\
I_{1,7} &= I_{1,8} = \frac{1}{8}\big[\langle D^2\rangle I_1(0)R_1^2(2\tau) + \langle DE\rangle I_2(0)R_1(2\tau)R_2(2\tau)\big] \\
I_{2,7} &= I_{2,8} = \frac{1}{8}\big[\langle E^2\rangle I_2(0)R_2^2(2\tau) - \langle DE\rangle I_1(0)R_1(2\tau)R_2(2\tau)\big] \\
I_{2,9} &= -\frac{1}{2}I_2(0)\big[\langle F^2\rangle R_2^2(2\tau)\big],
\end{aligned}
\qquad [17]
$$

with

$$
\begin{aligned}
D &= \frac{\omega_{13}}{\omega}\sin(2\pi J_\sigma\tau)\cos(\omega\tau) \\
E &= \frac{2\pi J_\delta}{\omega}\sin^2\left(\frac{\omega_{13}}{2}\tau\right) \\
F &= \sin^2\left(\frac{2\pi J_\sigma}{2}\tau\right),
\end{aligned}
\qquad [18]
$$

are smaller than those of the first eight lines. This is due to the fact that, except for the negative line located at $\Omega_9 = \sigma_{13}$, they are all scaled by $\frac{2\pi J_\delta}{\omega}$, which is a small parameter for typical values of the J coupling constants between carbon nuclei.

For practical applications, thus, only the dominant lines given by Eq. [14] are considered. Again, the values of the involved J couplings are taken from solution NMR spectra or from solid state NMR experiments designed for measurements of J couplings (i.e., the TOBSY sequence (*18*)), so that the only unknown parameters are the relaxation functions $R_p(2\tau)$, with $p = 1, 2, 3$. As a general feature, the dependencies on the dipolar coupling, ω_{13}^{D}, and on relaxation parameters are more complex now than in the spin-pair case. Nevertheless, performing the summation of all DQ slices, and taking the ratio between the dipolar and J lines, one gets

$$
\begin{aligned}
\eta &= \frac{I_{1,1} + I_{3,1}}{I_{1,2} + I_{2,2} + I_{2,3} + I_{3,3}} \\
&= \frac{1}{4}\frac{\langle A^2\rangle(1 + r_{31})^2}{\left\langle\left(B_+ + \frac{1}{2}C_+r_{21}\right)\right\rangle^2\left\langle\left(B_- + \frac{1}{2}C_-r_{21}\right)\right\rangle^2},
\end{aligned}
\qquad [19]
$$

which is less sensitive to errors determined by uncertainties in the measurement of the relaxation times. In the ideal case when all the nuclear sites are characterized by relaxation times whose

values are close to each other, one finds that the values of all possible ratios $r_{jk} = R_j/R_k$ are close to 1. In this case there is only a marginal influence of relaxation upon the measured parameter, η. However, even in the other extreme, when the difference between the relaxation times is large, the use of the dimensionless parameters r_{jk}, whose values can be approximated by the ratio between the corresponding linewidths, is expected to lead to a more accurate evaluation of the dipolar coupling ω_{13}^{D}, than in the case when the absolute values of the relaxation functions are employed. Similar to the spin-pair case, the same restriction to a small difference between the relaxation times of the R^2 recoupled sites also applies here. For the particular example investigated above, this condition translates to $r_{13} \simeq 1$.

To include also the case of ^{1}H R^2-DQ spectra in the theory, we briefly analyze below a three-spin system made up of one spin with the resonance frequency ω_1 and two spins with ω_2. Distinct features occur now in the resulting spectrum, which can be better understood if the effect of J coupling is disregarded. Thus, only the dipolar terms in the expression of the Hamiltonian [3] are considered here, and, for simplicity, the two coupling constants are assumed to be equal to each other, that is, $\omega_{12}^{\mathrm{D}} = \omega_{13}^{\mathrm{D}} = \omega^{\mathrm{D}}$.

Following the same procedure described in the previous section, the structure of the corresponding R^2-DQ spectrum can be easily evaluated. The four-peak pattern, with absorption lines located at $\sigma_{12} \pm \delta_{12}$ along the DQ dimension, characterizes this spectrum as well, but, in addition, one obtains also absorption peaks located at σ_{12} and $\sigma_{12} \pm 2\delta_{12}$. This resembles the sidebands pattern structure obtained in MQ MAS spectra (*12*), which can be used for measuring the dipolar coupling ω^{D}, for instance, from the ratio between the first order sidebands and the central line, i.e.,

$$\eta = \frac{I_{1,1} + I_{2,1}}{I_{1,2} + I_{2,2}} = \frac{1}{4} \frac{\langle (3\sin(\sqrt{2}\omega_{12}\tau) + \sin(2\sqrt{2}\omega_{12}\tau))^2 \rangle}{\left\langle \left(8\sin^2\left(\frac{\sqrt{2}}{2}\omega_{12}\tau\right) + \sin^2(2\sqrt{2}\omega_{12}\tau)\right)^2 \right\rangle}. \quad [20]$$

Thus, distinct from the case of ^{13}C spectra, the J lines are no longer needed here as a reference for the dipolar lines in order to determine the dipolar coupling, because this can be extracted in a more direct and simple way from the sideband pattern determined solely by the dipolar interaction. Indeed, if also the J terms are considered in Eq. [3], the corresponding expression of η depends in a much more complex way on both interaction parameters.

For a quantitative analysis of the ^{1}H R^2-DQ spectra it is thus preferable to employ such experimental conditions for which the dipolar sideband pattern is not too much affected by the J coupling interaction. In principle, this holds in the limit of short excitation times, provided that $J\tau \ll 1$. Fortunately, due to the relatively small values of J coupling constants in proton systems, the above requirement is well satisfied for the smallest value of τ that can be employed in our experiment, i.e., $\tau = \tau_{\mathrm{R}}$.

Finally, one mentions that, although necessary, the short excitation time limit is not sufficient for neglecting the J coupling from analysis. Whether such an approximation can be used depends also on the relative values between the J coupling constants and the R^2 recoupled dipolar interaction. Two distinct situations must be distinguished now. In the case of those j and k spins which are subjected to rotational resonance, additionally one must fulfill the requirement $2\pi J_{jk} \ll \omega_{jk}^{\mathrm{D}}$. For any other J couplings, J_{jl}, with $l \neq k$, such a condition is not needed in principle, because the corresponding J lines and the dipolar lines do not overlap.

4. RESULTS AND DISCUSSION

A first comparison between the theoretical and experimental results clearly indicates that the truncation of the interaction Hamiltonian to its static terms can very well explain the prominent features of the recorded R^2-DQ spectra. For a rigorous analysis, however, also the effect of the rotor-modulated terms, like chemical shift anisotropy and off-R^2 dipolar couplings, must be appropriately taken into account. Such an extension of the theory is beyond the purpose of the present investigation, so that below we only provide a qualitative discussion about the importance of this effect.

During the excitation/reconversion periods there are two distinct mechanisms by which the rotor-modulated terms are averaged out, namely the scaling of these terms with increased powers of the spinning frequency (*31*) and the rotor synchronization of the excitation/reconversion times. During the DQ evolution period, however, only the first mechanism is present. As demonstrated previously, this mechanism alone can efficiently average out the rotor-modulated spin interactions provided that the fast MAS condition is fulfilled. As a criterion for this limit, one can take, for instance, the requirement that the strongest coupling parameter associated to the rotor-modulated terms must be smaller than the spinning frequency (*31*).

4.1. The ^{13}C Three-Spin System in L-Alanine

In the case of ^{13}C nuclei in L-alanine, the strongest rotor-modulated contribution comes from the CSA term corresponding to the COOH carbon. Here, the ratio $\delta_3^a/\omega_{\mathrm{R}} \simeq 3/5$, with δ_3^a kHz—the CSA coupling constant (*33*), fits rather well the condition for fast MAS. Therefore, the discussion of the ^{13}C R^2-DQ spectrum in Fig. 2 is straightforward, since the theoretical results obtained in the case of the three-spin system can be directly applied for its quantitative analysis. Consequently, for the evaluation of the dipolar coupling ω_{13}^{D}, one first adds together all three DQ slices. The resulting 1D DQ spectrum is then used to determine the ratio η between the integral intensities of the dipolar and J lines. Finally, the experimental value, $\eta = 0.48$, is inserted in Eq. [19], where, besides ω_{13}^{D}, all the other parameters are considered known. Specifically, $J_\sigma = 45$ Hz and $J_\delta = 10$ Hz result using the J coupling constants J_{12} and J_{23} given in

Ref. (*28*), while the ratios between the specified relaxation functions have been approximated by $r_{21} = \Delta\nu^{(2)}/\Delta\nu^{(1)} = 1.71$ and $r_{31} = \Delta\nu^{(3)}/\Delta\nu^{(1)} = 1.05$. The $\Delta\nu^{(j)}$ are the linewidths of the specified absorption lines, measured away from any R^2 condition: here we employed $\nu_R = 25$ kHz. The value of the dipolar coupling, $\omega_{13}^D = 450$ Hz, obtained using this procedure, agrees very well with the value of 460 Hz that corresponds to the known COOH–CH_3 internuclear distance (*33*). Figure 2 is a nice illustration of the benefits of on and off-rotational resonance conditions in terms of stepwise assignment (off-rotational resonance) and assignment plus internuclear distance estimation (on-rotational resonance).

4.2. ^{1}H Residual Dipolar Interactions in Crosslinked Natural Rubber

The ^{1}H R^2-DQ spectra presented in Fig. 3 can no longer be analyzed using Eq. [20]. According to the discussion in the previous section, for a more accurate evaluation of the residual dipolar couplings (*32*) between the CH and CH_2 protons, $\bar{\omega}_{12}^D$, or between the CH and CH_3 protons, $\bar{\omega}_{13}^D$, it is preferable to employ the short excitation time limit. Considering now the values of J_{12} and J_{13} given in Section 2, one obtains $J_{12}\tau_R \simeq 1/751$ and $J_{13}\tau_R \simeq 1/1700$, respectively. That is, using $\tau = \tau_R$, the first requirement for the short excitation time approximation, $J\tau \ll 1$, is fulfilled in both cases.

The results of the experiments performed at $\tau = \tau_R$ are illustrated in Fig. 4, in the form of 1D R^2-DQ spectra, which are obtained by adding all DQ slices in the corresponding 2D spectra. The sideband pattern predicted by theory can be easily identified in both cases. A quantitative analysis will be considered, however, only for the spectrum obtained under the R^2 condition with respect to the CH–CH_2 lines (Fig. 4a), since only this case approaches the theoretical model presented in the previous section.

For ^{1}H nuclei in elastomers, the strongest contribution of the rotor-modulated terms comes from the proton–proton dipolar interaction inside the CH_2 functional group. Using the value $\bar{\omega}_{CH_2}^D \simeq 300$ Hz (*32*) of the corresponding residual dipolar coupling, one obtains $\bar{\omega}_{CH_2}^D/\omega_R = 0.2$, which indicates that the fast MAS approximation applies also here. Nevertheless, distinct from the ^{13}C spectra, in the case of protons there is another effect which limits the accuracy in evaluating dipolar couplings based on the three-spin model presented above. Specifically, here one should take into account that, besides the dipolar interaction of the CH proton with the nearest CH_2 protons, also the interactions with the next nearest neighbors will encode to some extent the resulting R^2-DQ spectrum. Therefore, the value $\bar{\omega}_{12}^D = 220$ Hz obtained using Eq. [20] must be considered within the error limits introduced by neglecting the multispin character of the investigated system. As in the case of the carbon spectrum, this value was determined by inserting the experimental ratio, $\eta = 1.4$, into its corresponding theoretical expression, Eq. [20]. Finally, comparing this value of $\bar{\omega}_{12}^D$ with J_{12}, one can see that also the second requirement for the short excitation time approximation is satisfied for this spectrum.

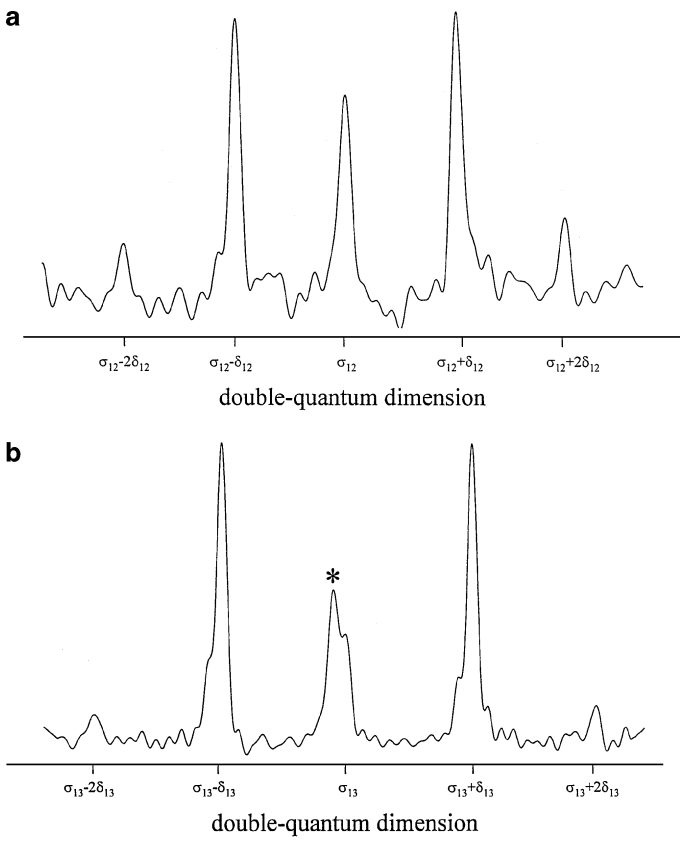

FIG. 4. (a) The 1D R^2-DQ spectrum of ^{1}H in natural rubber (phr = 1), obtained by adding together all DQ slices of the corresponding 2D spectrum. It was recorded under the $n = 1$ R^2 condition corresponding to the CH–CH_2 lines, using a total excitation time of $2\tau = 2\tau_R = 1.31$ ms. (b) Similar to case (a), except that the $n = 1$ R^2 condition corresponding to the CH–CH_3 lines is employed. The absorption line marked with an asterisk originates from the J coupling between the CH–CH_2 protons.

In a similar way one can analyze also the sideband pattern in Fig. 4b, which corresponds to the R^2 condition with respect to the CH–CH_3 lines. Here we refrain from a quantitative evaluation of the corresponding dipolar coupling: this requires the extension of the theoretical model to a six-spin system, whose investigation is far beyond the purpose of the present investigation. However, a qualitative discussion of the result is still possible. For instance, compared with the previous spectrum, the ratio between the intensity of the central line and the first-order sidebands is smaller now, which basically reflects a reduced value of the CH–CH_3 dipolar coupling. This result is not surprising, taking into account the increased CH–CH_3 distance. Due to the r^{-3} distance dependence of the dipolar coupling, it is even expected that $\bar{\omega}_{13}^D$ is several times smaller than $\bar{\omega}_{12}^D$. Based on this conclusion, one can also explain the reason why the effect of the J_{CH-CH_2} coupling is no longer negligible here, as can be judged from the rather large intensity of the corresponding J line (marked with an asterisk in Fig. 4b).

5. CONCLUSION

The major difficulty in applying the rotational resonance techniques for structural investigations in rotating solids is determined by their increased sensitivity to relaxation parameters, in addition to the measured dipolar coupling. This particularly holds in the case of weakly coupled nuclear spins, that is, exactly those cases which are important for practical applications. In the present work we introduce a new R^2-DQ technique where the influence of relaxation upon the measured parameters is much reduced, thus leading to increased accuracy in the evaluation of dipolar couplings.

The theory necessary for the basic understanding of the resulting 2D R^2-DQ spectra is derived by confining the analysis to the static terms of the interaction Hamiltonian under R^2 conditions. With the help of the theoretical models and the experimental examples treated, it is shown that even a quantitative analysis is possible under this approximation, provided that the condition for the fast MAS regime is fulfilled. For a discussion of the fast MAS see, for instance, Ref. (*31*). In this limit, the contribution of the rotor-modulated terms, i.e., chemical shift anisotropy and off-R^2 dipolar couplings, can be neglected in a first approximation, which leads to a simplified spectral analysis. For a more rigorous description, an extension of the theoretical description is required which includes also the effect of such rotor-modulated terms. Such an extension will be reported elsewhere, because it is beyond the purpose of this work, which is intended to provide physical insights into the structure of the resulting R^2-DQ spectra.

The potential for practical applications of this method is demonstrated by the examples of ^{13}C and ^{1}H R^2-DQ spectra recorded in uniformly ^{13}C labeled L-alanine and a crosslinked natural rubber. In the first case, which corresponds to the most common application of rotational resonance techniques in biochemical structural investigations, it is shown that the proposed method is well adapted for use in uniformly labeled compounds. The agreement between the internuclear distance measured by the proposed method and the previously reported value shows that not only the influence of relaxation is small here, but also the contribution of CSA. Nevertheless, for biomolecules the distances of interest are usually between sites that have a negligible mutual J coupling. The new R^2 DQ technique discussed above is advantageous in these cases because of the reduced effect of relaxation.

The latter example demonstrates, for the first time, that the application of the R^2 phenomenon is not confined to rare isotopes in rigid biomolecules, but can be also used for determining small proton–proton residual dipolar couplings between different functional groups in soft solids. The short excitation / reconversion time limit, which was found to be important in proton systems, can be used in addition for simplifying the multispin dipolar network.

In conclusion, it is emphasized that the use of this method is attractive in high magnetic fields. The dipolar network topology is expected to further simplify here, because the fast MAS regime under R^2 dipolar recoupling is easier to reach at high magnetic fields.

ACKNOWLEDGMENTS

This work was supported by a grant from the Bundesministerium für Bildung und Forschung (BMBF) under German–Israeli Project Cooperation (DIP). Helpful discussions with Prof. Hans W. Spiess and Dr. Ingo Schnell in the early stages of this project are gratefully acknowledged. C.F. thanks the Deutsche Forschungsgemeinschaft for financial support from a visiting scientist grant and the Romanian National Agency of Science (ANSTI).

REFERENCES

1. A. E. Bennett, R. G. Griffin, and S. Vega, Recoupling of homo- and heteronuclear dipolar interactions in rotating solids, *in* "Solid-State NMR IV: Methods and Applications of Solid State NMR," Vol. 33, "NMR Basic Principles and Progress," p. 1, Springer-Verlag, Berlin, 1994.
2. E. R. Andrew, A. Bradbury, and R. G. Eades, NMR from a crystal rotated at high speeds, *Nature* **182,** 1659 (1958).
3. I. J. Lowe, Free induction decays in rotating solids, *Phys. Rev. Lett.* **2,** 285–287 (1959).
4. R. Tycko and G. Dabbagh, Measurement of nuclear magnetic dipole–dipole couplings in magic angle spinning NMR, *Chem. Phys. Lett.* **173,** 461–465 (1990).
5. R. Tycko and G. Dabbagh, Double-quantum filtering in magic-angle-spinning NMR spectroscopy: An approach to spectral simplification and molecular structure determination, *J. Am. Chem. Soc.* **113,** 9444–9448 (1991).
6. N. C. Nielsen, H. Bildsøe, H. J. Jakobsen, and M. H. Levitt, Double-quantum homonuclear rotary resonance: Efficient dipolar recovery in magic-angle spinning nuclear magnetic resonance, *J. Chem. Phys.* **101,** 1805–1812 (1994).
7. Y. K. Lee, N. D. Kurur, M. Helmle, O. G. Johannessen, N. C. Nielsen, and M. H. Levitt, Efficient dipolar recoupling in the NMR of rotating solids, *Chem. Phys. Lett.* **242,** 304–309 (1995).
8. M. Hohwy, H. J. Jakobsen, M. Edén, M. H. Levitt, and N. C. Nielsen, Broadband dipolar recoupling in the nuclear magnetic resonance of rotating solids, *J. Chem. Phys.* **108,** 2686–2694 (1998).
9. C. M. Rienstra, M. E. Hatcher, L. J. Mueller, B. Sun, S. W. Fesik, and R. G. Griffin, Efficient multispin homonuclear double-quantum recoupling for magic-angle spinning NMR: ^{13}C–^{13}C correlation spectroscopy of U-^{13}C-erythromycin A, *J. Am. Chem. Soc.* **120,** 10602–10612 (1998).
10. M. Hohwy, C. M. Rienstra, C. P. Jaroniec, and R. G. Griffin, Fivefold symmetric homonuclear dipolar recoupling in rotating solids: Application to double quantum spectroscopy, *J. Chem. Phys.* **110,** 7983–7992 (1999).
11. A. Brinkmann, M. Edén, and M. H. Levitt, Synchronous helical pulse sequences in magic-angle spinning NMR. Double-quantum recoupling of multiple-spin systems, *J. Chem. Phys.* **112,** 8539 (2000).
12. R. Graf, D. E. Demco, J. Gottwald, S. Hafner, and H. W. Spiess, Dipolar couplings and internuclear distances by double-quantum nuclear magnetic resonance spectroscopy of solids, *J. Chem. Phys.* **106,** 885–895 (1997).
13. N. C. Nielsen, F. Creuzet, R. G. Griffin, and M. H. Levitt, Enhanced double-quantum nuclear magnetic resonance in spinning solids at rotational resonance, *J. Chem. Phys.* **96,** 5668–5677 (1992).
14. P. C. Costa, B. Sun, and R. G. Griffin, Rotational resonance tickling: Accurate internuclear distance measurements in solids, *J. Am. Chem. Soc.* **119,** 10821–10830 (1997).

15. Y. S. Balasz and L. K. Thompson, Practical methods for solid-state NMR distance measurements on large biomolecules: Constant-time rotational resonance, *J. Magn. Reson.* **139,** 371–376 (1999).
16. T. Karlsson, M. Edén, H. Luthman, and M. H. Levitt, Efficient double-quantum excitation in rotational resonance NMR, *J. Magn. Reson.* **145,** 95–107 (2000).
17. S. Dusold and A. Sebald, Double-quantum filtration under rotational-resonance conditions: Numerical simulations and experimental results, *J. Magn. Reson.* **145,** 340–356 (2000).
18. M. Baldus and B. H. Meier, Total correlation spectrocopy in the solid state. The use of scalar couplings to determine the through-bond connectivity, *J. Magn. Reson. A* **121,** 65–69 (1996).
19. D. P. Raleigh, M. H. Levitt, and R. G. Griffin, Rotational resonance in solid state NMR, *Chem. Phys. Lett.* **146,** 71–76 (1988).
20. M. Maricq and J. S. Waugh, NMR in rotating solids, *J. Chem. Phys.* **70,** 3300–3316 (1979).
21. F. Creuzet, A. McDermott, R. Gebhard, K. van der Hoef, M. B. Spijker-Assink, J. Herzfeld, J. Lugtenburg, M. H. Levitt, and R. G. Griffin, Determination of membrane protein structure by rotational resonance NMR: Bacteriorhodopsin, *Science* **251,** 783–786 (1991).
22. J. M. Griffiths, T. T. Ashburn, M. Auger, P. R. Costa, R. G. Griffin, and P. T. Lansbury, Rotational resonance solid-state NMR elucidates a structural model of pancreatic amyloid, *J. Am. Chem. Soc.* **117,** 3539–3546 (1995).
23. P. R. Costa, D. A. Kocisko, B. Q. Sun, P. T. Lansbury, and R. G. Griffin, Determination of peptide amide configuration in a model amyloid fibril by solid-state NMR, *J. Am. Chem. Soc.* **119,** 10487–10493 (1997).
24. X. Feng, P. J. E. Verdegem, Y. K. Lee, M. Helmle, S. C. Shekar, H. J. M. de Groot, J. Lugtenburg, and M. H. Levitt, Rotational resonance NMR of $^{13}C_2$-labelled retinal: Quantitative internuclear distance determination, *Solid State NMR* **14,** 81–90 (1999).
25. M. H. Levitt, D. P. Raleigh, F. Creuzet, and R. G. Griffin, Theory and simulations of homonuclear spin pairs in rotating solids, *J. Chem. Phys.* **92,** 6347 (1990).
26. T. Nakai and C. A. McDowell, An analysis of NMR spinning sidebands of homonuclear two-spin systems using Floquet theory, *Mol. Phys.* **77,** 569–584 (1992).
27. A. Schmidt and S. Vega, The Floquet theory of nuclear magnetic resonance spectroscopy of single spins and dipolar coupled spin pairs in rotating solids, *J. Chem. Phys.* **96,** 2655–2680 (1992).
28. T. Fujiwara, P. Khandelwal, and H. Akutsu, Compound radiofrequency-driven recoupling pulse sequences for efficient magnetization transfer by homonuclear dipolar interaction under magic-angle spinning conditions, *J. Magn. Reson.* **145,** 73–83 (2000).
29. M. Hesse, H. Meier, and B. Zeeh, "Spektroskopische Methoden in der Organischen Chemie," Thieme, Stuttgart, 1995.
30. M. Helmle, Y. K. Lee, P. J. E. Verdegem, X. Feng, T. Karlsson, J. Lugtenburg, H. J. M. de Groot, and M. H. Levitt, Anomalous rotational resonance spectra in magic-angle spinning NMR, *J. Magn. Reson.* **140,** 379–403 (1999).
31. C. Filip, S. Hafner, I. Schnell, D. E. Demco, and H. W. Spiess, Solid-state magnetic resonance spectra of dipolar-coupled multi-spin systems under fast magic angle spinning, *J. Chem. Phys.* **110,** 423–439 (1999).
32. M. Schneider, L. Gasper, D. E. Demco, and B. Blümich, Residual dipolar couplings by ^{1}H dipolar-encoded longitudinal magnetization, double- and triple-quantum nuclear magnetic resonance in cross-linked elastomers, *J. Chem. Phys.* **111,** 402–415 (1999).
33. A. Naito, S. Ganapathy, A. Akasaka, and C. A. McDowell, Chemical shielding tensor and ^{13}C–^{14}N dipolar splitting in single crystals of L-alanine, *J. Chem. Phys.* **74,** 3190–3197 (1981).